

CRITICAL STATE OF KEUPER MARL SILT

by

Aminaton Bt Marto, PhD
Faculty of Civil Engineering
Universiti Teknologi Malaysia

ABSTRACT

Research has been carried out to establish an experimentally based effective stress volumetric compression model for isotropically and anisotropically consolidated Keuper marl silt subjected to undrained cyclic loading with drainage rest-periods [Marto (1996)]. The experimental programme included monotonic strain controlled triaxial tests and three stages of undrained two-way cyclic loading with drained rest-periods. The monotonic strain controlled triaxial tests on both isotropically and anisotropically, normally and overconsolidated silt were carried out to establish the critical state boundary surface of the soil. This critical state boundary surface was used as a framework for cyclic loading tests. This paper will discuss the development of critical state parameters and the critical state boundary surface for the investigated material.

INTRODUCTION

During shearing, soils ultimately reach a critical state where they continue to distort with no change of state (i.e at constant deviator stress (q), constant mean normal effective stress (p') and constant water content) as can be seen in Figure 1. Before the critical state there may be a peak state and after large strains clay soils reach a residual state. The peak state is associated with dilation and the residual state is associated with laminar flow. Figure 2 (a) and (b) show the critical state line (CSL) obtained from drained and undrained triaxial tests. These figures show that, at the critical state, there is a unique relationship between the deviator stress and mean normal effective stress, the mean normal effective stress and the specific volume (v). The critical state lines are given by:

$$q_f = Mp'_f \quad (1)$$

$$v_f = \Gamma - \lambda \ln p'_f \quad (2)$$

where the subscripts 'f' denote ultimate failure at the critical states. The critical stress ratio, M , is equivalent to the critical friction angle ϕ'_c . In Figure 2 (b) the gradients of the critical state line and the isotropic normal consolidation line are λ and the lines are parallel and the gradient of the critical state line is the same for triaxial and extension. For the parameters M and Γ , however, it is necessary to use subscripts 'c' and 'e' to distinguish between critical state, in compression and extension, and for most soils the value of both Γ_c and Γ_e , and M_c and M_e differ. The parameters λ , Γ and M (or ϕ') for triaxial compression are regarded as constants for a particular soil and values for some typical soils are given in Table 1. However, these critical state parameters can also be estimated from the classification test parameters, particularly the Atterberg Limit [Atkinson (1993)]. At the critical state soils are essentially perfectly frictional and the cohesion c' can be neglected.

MATERIAL AND PROCEDURE

The material used in this research was "Keuper Marl", the name given to a particular series of rocks laid down in the British Isles during the late Triassic Period. It is widely found throughout the British Isles whereby the erosions of the overlying Jurassic and Cretaceous formations has exposed a band of heavily overconsolidated Keuper marl stretching from Somerset to Cleveland. The outcrop continues on the sea bed for some distance off the Northumberland Coast [Conn (1988)]. This material is also found as a subsurface deposit over large areas of the southern North Sea [Pegrum, Ress and Naylor (1975)]. These deposits of thickness between 200 - 400 metres comprise a variety of rock types, but primarily red brown to green mudstones and shales, generally referred as "Marl" [Kolbuszewski, Birch and Shojobi (1965)].

The material, supplied in dried powdered form, was the plastic silt fraction (passing 63 μ m) having $G_s = 2.66$, $w_L = 36\%$, $w_p = 17\%$ and $PI = 19\%$. In order to establish the critical state boundary surfaces and the critical state parameters for the investigated material, four test series have been performed; isotropic consolidation, anisotropic consolidation, monotonic triaxial compression and monotonic triaxial extension. The test series are shown in Tables 2 to 4. The material was initially one-dimensionally consolidated at 80 kPa from a slurry prepared to twice the liquid limit. The consolidation was usually completed after about five days. Samples from the moulds were then

extruded to make samples 76mm by 38mm which were mounted in a Bishop and Wesley stress path cell with porous stones at each end and spiral filter drains. Samples were saturated under a back pressure of 200 kPa and any samples which did not reach a B value of at least 0.97, were discarded. The stress path cell was linked to a computer via three digital pressure controllers and a digital pressure interface to control and measure axial load, deformation, volume change, cell pressure and pore pressure (Figure 3). The equipment system is called Geotechnical Digital System (GDS) [Menzies (1988)] and was used throughout this research work.

In determining the location of the normal consolidation line, swelling and recompression line, two samples were initially isotropically consolidated, allowed to swell and then recompressed. Other results were later taken from the moisture content measured at the end of the tests for fourteen monotonic triaxial samples. Similarly, two samples were also initially anisotropically consolidated to establish the K_0 -line and swelling line of the soil. Sixteen more results were taken from the moisture contents at the end of monotonic tests to establish a better fit for the lines in question.

In monotonic triaxial tests, isotropically and anisotropically consolidated samples were performed at different stress histories, i.e. at 1, 2, 4 and 40. Axial deformation control was used with a compression or extension rate of ± 5 mm/hr and the tests ended after the sample had reached ± 20 % axial strain. The test period was about 3 hours.

DEFINITION OF STATE PARAMETERS

The state parameters q and p' are defined as :

$$q = \sigma'_1 - \sigma'_3 \quad (3)$$

$$p' = (\sigma'_1 + 2 \sigma'_3)/3 \quad (4)$$

where

- q - deviator stress
- p' - mean normal effective stress
- σ'_1, σ'_3 - major and minor effective principle stresses

The chosen normalising pressure is p'_e and known as an equivalent pressure, i.e. the value of p' at the point on normal consolidation line at the same specific volume. Normalising the effective stresses, p' and q , with respect to this equivalent pressure will allow results from samples with different overconsolidation ratios to be brought onto a single plane.

RESULTS AND ANALYSIS

Isotropic Consolidation

The normal consolidation line (NCL), swelling line (SL) and recompression line (RL) of the silt soil were initially located from two continuous isotropic consolidation tests (IC1 and IC2). The moisture content taken at the end of the tests enabled the specific volume at a particular mean normal effective stress of the soil to be back figured. This was calculated from the value of the sample volume, recorded by the GDS system at the start of each consolidation pressure. By plotting the results from the two tests in $v - \ln p'$ space, the initial NCL, SL and RL can be visualised as shown in Figure 4. The NCL and SL are linear lines whereas the RL is a curve.

The NCL obtained earlier in Figure 4 was later refined by adding eleven more results from consolidated undrained (monotonic) triaxial tests. This can be seen in Figure 5(a). From the regression analysis, the slope of the NCL ($-\lambda$) was found to be -0.083 and the line crossed the $p' = 1$ axis at $v = 2.062$. (This v obtained at $p' = 1$ is defined as N). Later results added from the moisture content of specimens after undergoing cyclic loading, were found to have no effect on the regression value.

Similar to the NCL, the SL was also determined after adding the results from moisture contents taken at the end of monotonic triaxial tests, in this case from ten overconsolidated samples. Regression analysis on the plot of specific volume against $\ln p'$ gave the results as shown in Figure 5(b). The slope of the SL ($-\kappa$) was found to be -0.02. Additional results obtained from samples after undergoing cyclic loading tests which were added to the plot, did not alter the slope of the SL, as in the case of the NCL.

Considering the RL, the test results shown in Figure 4 did not give a similar straight line as in the case of SL, when plotted in $v - \ln p'$ space. The literature review [Wroth and Houlsby (1985)] suggested that the recompression behaviour is often treated as a straight line, similar to the SL. Incorporating the additional data obtained at a later stage of the research work the RL was re-plotted as a log-log function and found to be a straight line with a slope (given

a symbol $-\zeta$) of -0.0141 (Figure 6(b)). Earlier work by Butterfield (1979) also suggested similar way of plotting the graph.

Anisotropic Consolidation

The anisotropic (K_0) consolidation tests performed on the silt specimens gave the K_0 line in $q - p'$ space as shown in Figure 7. Figure 7(a) shows the results obtained from the two initial anisotropic tests (AC1 and AC2). The effective stress points for all the specimens forms a unique straight line with $q/p' = 0.73$ giving an average K_0 value of 0.51. However, with the addition of more results from the monotonic tests carried out on anisotropic samples, the average slope of q/p' was found to be 0.71, therefore $K_0 = 0.52$ (Figure 7(b)). This value is exactly the same as that obtained by Overy (1982), who worked on anisotropically consolidated silty clay Keuper Marl, although the method of obtaining K_0 was quite different. However, Okorie (1991) found a value of 0.58 - 0.62 from his work on silt sized Keuper Marl samples.

A plot of specific volume against mean normal effective stress for a typical anisotropically consolidated silt specimen is shown in Figure 8. As in isotropic consolidation, the points on the graph were obtained by calculation from the final moisture content of the soil at the end of testing. The normally consolidated part of the graph becomes linear for a mean normal effective stress greater than 60 kPa. Since the sample was initially one-dimensionally consolidated from a slurry under 80 kPa vertical stress, then if the K_0 value is 0.52, p' was 55 kPa at this stage. The soil was therefore initially in an overconsolidated state until the preconsolidation pressure of 55 kPa was exceeded, hence forming a curve in the early part of the graph.

As can be seen in Figure 8, the slope of the K_0 normal consolidation line (K_0 NCL), was found to be -0.0845, i.e. slightly steeper than the NCL obtained from isotropic consolidation. Overy (1982) found that the slope of this line was -0.0866, in his work on silty clay (Keuper Marl), which was close to the author's result. However, Okorie (1991) obtained a much less value of this K_0 NCL slope in his work on Keuper Marl silt. The variation might be explained by the difference in the chosen applied vertical pressure when consolidating the slurry for obtaining the specimens for triaxial testing. Another reason might come from the difference in the particle size distributions of the silt used.

Since K_0 NCL was found to have a slightly different slope as the NCL's the lines are plotted using an average value in Figure 9. From this Figure, it can be seen that this K_0 NCL lies in between the NCL and the CSL, as predicted by the critical state theory of Schofield and Wroth (1968). The K_0 NCL crosses the $p' = 1$ axis at $v = 2.054$. (This v value is defined as N_{k0}). The swelling line in anisotropic consolidation is also reasonably linear (AB in Figure 8) when plotted in $v - \ln p'$ space. It has similar slope to the swelling line obtained from isotropic consolidation tests which was -0.02 .

STRESS PATH AND CRITICAL STATE LINE

Monotonic Compression

Failure states of consolidated undrained compression tests on isotropically and anisotropically consolidated samples of various stress histories are plotted in $q - p'$ space and $v - p'$ space in Figure 10. Plotted together, these data points define a single straight line through the origin in $q - p'$ space and a single curved line in $v - p'$ space whose shape is similar to the normal consolidation line. This single and unique line of failure points is defined as the 'critical state line' (CSL) [Atkinson and Bransby (1978)]. Its crucial property is that failure of initially isotropically and anisotropically consolidated samples will occur once the stress states of the samples reach the line, irrespective of the test path followed by the samples on their way to the critical state line. Failure will be manifested as a state at which large shear distortions occur with no change in stress, or in specific volume.

The projection of the critical state line onto the $q - p'$ plane in Figure 10 is described earlier by Equation 1. From a linear least squares regression analysis, M was found to be 1.16. With a known M value, the angle of internal friction for compression, ϕ'_c , can be calculated from the equation [Atkinson and Bransby (1978)] :

$$M = \frac{6 \sin \phi'_c}{(3 - \sin \phi'_c)} \quad (5)$$

Therefore,

$$\phi'_c = \sin^{-1} \frac{3M}{6 + M}$$

and for $M = 1.16$, $\phi'_c = 29^\circ$

The projection of the critical state line onto the $v - p'$ plane in Figure 10 is curved. However, if the same data are replotted with axes $v - \ln p'$, the points fall close to a straight line, as shown in Figure 11. A regression analysis shows that the gradient of this line is the same as the gradient of the corresponding normal consolidation line discussed earlier. The critical state line in Figure 11 is described earlier by Equation 2. Γ is defined as the value of v corresponding to $p' = 1$ kPa on the critical state line and $-\lambda$ is the slope of critical state line. From Figure 11, it can be seen that $\Gamma = 2.023$ and $\lambda = 0.083$.

Equations 1 and 2 together define the position of the critical state line in $q : p' : v$ space; M and Γ , like N , λ and κ are regarded as soil constants.

The effective stress paths plotted in $q - p'$ space for both isotropically and anisotropically consolidated samples are shown in Figure 12. For normally consolidated samples, it can be seen that the shape of the stress paths are similar, suggesting that all curves could be collapsed into one by plotting q/p'_e against p'/p'_e . The stress path for normally isotropically consolidated samples starts from the normal consolidation line where $q = 0$ and $p' = p'_c$ (p'_c is effective consolidation pressure). As the sample is sheared undrained in compression, the applied stress path travels upwards and to the right along a line rising at $\tan^{-1} 3$. Positive pore pressures are produced which cause the effective stress path to rise to the left along a curved path. When the path reaches the peak value, the sample will continue to suffer plastic deformation with no change in the applied stresses or measured pore pressure. As for the anisotropically consolidated specimens, the stress path starts from the K_0 line where q already has some value at the beginning of the compression. The effective stress paths for normally anisotropically consolidated specimens are similar to the isotropically consolidated specimens whereby the stress paths rise to the left along a curved path until reaching a peak value, where failure occurred.

The curved surface traced out in $q' : p' : v$ space by families of drained and undrained tests is identical for both families of tests. The same surface is followed by all isotropically normally consolidated samples which are loaded by axial compression in the triaxial apparatus, as can be seen in Figure 12. This surface is called the 'Roscoe surface', and separates states which samples can achieve from states which samples can never achieve, and therefore is also known as a state boundary surface [Atkinson and Bransby (1978)].

For the isotropically overconsolidated specimens, the stress paths start from some point on the p' axis where $p' < p'_c$. During undrained compression the effective stress path travels vertically until it reaches the yield boundary. It then travels on the yield surface towards the critical state point, which was found to occur at $q/p'_e = 0.8$ and $p'/p'_e = 0.69$. Most of the overconsolidated specimens however failed on the yield surface before reaching the critical state point. This yield surface, known as 'Hvorslev surface' is also a state boundary surface [Atkinson and Bransby (1978)]. Roscoe, Schofield and Wroth (1958) suggested two reasons why the overconsolidated samples failed on the Hvorslev surface. Firstly, at the larger strains necessary to reach failure in overconsolidated samples, the assumption that the samples remain cylindrical is called into serious doubt. Secondly, errors due to membrane, side drain and plunger friction become accentuated at lower cell pressures. Atkinson and Bransby (1978) mentioned that the significant feature of the Hvorslev surface is that the shear strength of a specimen at failure is a function both of the mean normal stress, p' , and of the specific volume, v , of the specimen at failure. Results show that the linear Hvorslev surface in compression side for the investigated material, has an equation (Figure 12) :

$$\frac{q}{p'_e} = 0.26 + 0.78 \frac{p'}{p'_e} \quad (6)$$

The strain contours for isotropically and anisotropically consolidated specimens are plotted within the stress paths, shown respectively in Figure 13 and Figure 14, in an attempt to describe the strain behaviour of the specimens. It can be seen that for isotropically consolidated specimens, the strain contours are subhorizontal at low OCRs but they have a slope towards the origin at higher OCRs. As the samples approach failure they tend to become parallel to the failure envelope. These observations are similar to those made in Kaolin by Wroth and Loudon (1967) and by Parry and Nadarajah (1974) for low OCRs. Results are quite scattered for anisotropically consolidated specimens, but the trend of the strain contours are still the same as in isotropically consolidated specimens.

Monotonic Extension

The critical state line for extension tests is plotted in both the $q - p'$ space and $v - p'$ space, as shown in Figure 15. The gradient, M , of the critical state line projected onto the $q - p'$ plane is found to be 1.04. Using the equation of Atkinson and Bransby (1978), the angle of internal friction for extension, ϕ'_c can be calculated as follows :

$$M = \frac{6 \sin \phi'_e}{3 + \sin \phi'_e} \quad (7)$$

Therefore,

$$\phi'_e = \sin^{-1} \left(\frac{3M}{6 - M} \right)$$

and for $M = 1.04$,

$$\phi'_e = 37^\circ$$

The projection of the critical state line onto the $v - p'$ plane is curved (Figure 15), as observed in compression tests. When replotted with $v - \ln p'$ axes as shown in Figure 16, the line becomes linear with a similar gradient to the normal consolidation line. Using Equation 2 for the critical state line, i.e. $v_f = \Gamma - \lambda \ln p'_f$, Γ is found to be 2.026 and λ is equal to 0.083.

The effective stress paths for the extension tests are presented in Figure 17. The shape of the stress paths for both isotropically and anisotropically normally consolidated samples, looks the same. As expected, when the stress paths are plotted with deviator stress and mean normal effective stress normalised with respect to p'_e , they collapse onto one with critical state at $q/p'_e = -0.58$ and $p'/p'_e = 0.65$. The stress paths of the overconsolidated samples also travel to the critical state point but some failed at the Hvorslev surface, as was observed in compression tests.

The Hvorslev surface on the extension side has the equation :

$$\frac{q}{p'_e} = -0.2 - 0.59 \frac{p'}{p'_e} \quad (8)$$

The strain contours are as shown in Figure 18 and 19 for isotropically and anisotropically consolidated samples, respectively. The contours are in good agreement with those from compression tests. However it can be seen that the samples failed at higher strains in extension than in compression.

Critical State Boundary Surface

It has been shown earlier that the critical state point in compression is at $p'/p'_e = 0.69$ and $q/p'_e = 0.8$. In extension, the critical state point is at $p'/p'_e = 0.65$ and $q/p'_e = -0.58$. The Hvorslev surface on the compression side crosses the q/p'_e axis at 0.26, therefore the equation of the Hvorslev surface is $q/p'_e = 0.26 + 0.78 p'/p'_e$. On the extension side, the Hvorslev surface crosses

the q/p'_e axis at -0.2, and therefore the equation for the Hvorslev surface in extension is $q/p'_e = -0.2 - 0.59 p'/p'_e$. It is interesting to note that if both Hvorslev surfaces are continued beyond the q/p'_e axis they intersect on the p'/p'_e axis at -0.33 (Figure 20). A similar response was observed by Conn (1988) and Okorie (1991).

According to Wood (1990), there is a limit to the extent of the Hvorslev failure line at low values of p'/p'_e . It is supposed that the soil can withstand no tensile effective stresses, then the condition of zero effective radial stress defines a limiting line in triaxial compression OA in Figure 20, with OA having an equation:

$$q = 3p' \quad (9)$$

The condition of zero effective axial stress defined a limiting line in triaxial extension OB in Figure 20, where OB has an equation :

$$q = -\frac{3p'}{2} \quad (10)$$

The Hvorslev lines then span between the critical state points and the no-tension lines. The Hvorslev line in compression intersects the no-tension line at $q/p'_e = 0.35$, $p'/p'_e = 0.12$ while the Hvorslev line in extension intersects the no-tension line at $q/p'_e = -0.33$, $p'/p'_e = 0.22$. The complete critical state boundary surface for the investigated material is therefore as shown in Figure 21.

CONCLUSIONS

The slope of the normal consolidation line and the critical state line together with the failure envelope in compression and extension were the same for isotropically and anisotropically consolidated samples. The following critical state parameters for Keuper Marl silt were obtained:

$\lambda = 0.08$	$N = 2.062$	$\Gamma_e = 2.026$
$\kappa = 0.02$	$N_{Ko} = 2.054$	$M_c = 1.16$
$\zeta = 0.0141$	$\Gamma_c = 2.023$	$M_e = 1.04$

The critical state for triaxial compression tests was at $q/p'_e = 0.8$, $p'/p'_e = 0.69$ and for triaxial extension tests was at $q/p'_e = -0.58$, $p'/p'_e = 0.65$. The Hvorslev surfaces in compression and extension were linear.

REFERENCES

- [1] Atkinson, J.H. (1993). *An Introduction to The Mechanics of Soils and Foundations*, McGraw-Hill Book Company (UK) Ltd.
- [2] Atkinson, J.H. and Bransby, P.L. (1978). *The Mechanics of Soils, An Introduction to Critical State Soil Mechanics*, McGraw-Hill Book Company (UK) Ltd.
- [3] Butterfield, R. (1979). A Natural Compression Law for Soils (An Advance of $e - \log p'$), Technical Note, *Geotechnique*, Vol 29, No 4, 469 - 480.
- [4] Conn, G. M. (1988). *The Two-Way Repeated Loading of a Silty Clay*, PhD. Thesis, Loughborough University of Technology, UK.
- [5] Kolbuszczewski, J., Birch, N. and Shojobi, J. O. (1965). Keuper Marl Research, *Proceeding 6th International Conference on Soil Mechanics and Foundation Engineering*, Vol 1, 59 - 63.
- [6] Marto, A. (1996). *Volumetric Compression of a Silt under Periodic Loading*. PhD. Thesis, University of Bradford, UK.
- [7] Menzies, S. (1988). A Computer Controlled Hydraulic Triaxial Testing System, *Advanced Triaxial Testing of Soil and Rock*, ASTM STP 977, 82 - 94.
- [8] Okorie, A.D.O. (1991). *Cyclic Loading of Silt*. PhD. Thesis, University of Bradford, UK.
- [9] Overy, R.F. (1982). *The Behaviour of Anisotropically Consolidated Silty Clay under Cyclic Loading*, PhD. Thesis, University of Nottingham, UK.
- [10] Parry, R.H.G. and Nadarajah, V. (1974). Observations on Laboratory Prepared Lightly Overconsolidated Specimens of Kaolin, *Geotechnique*, Vol 24, 345 - 358.

- [11] Pegrum, R.M., Ress, G. and Naylor, D. (1975). *Geology of the North West European Continental Shelf, Vol 2 The North Sea*, Graham Trotman Dudley Ltd., London.
- [12] Roscoe, K.H., Schofield, A.N. and Wroth, C.P. (1958). *On the Yielding of Clays*, *Geotechnique*, Vol 8, No 1, 22 - 53.
- [13] Wroth, C.P. and Houlsby, G.T. (1985). *Soil Mechanics - Property Characterisation and Analysis Procedure*, Proc. 11th Int. Conf. on Soil Mechanics and Foundation Engineering, San Francisco, USA, Vol 1, 1 - 31.
- [14] Wroth, C.P. and Loudon, P.A. (1967). *The Correlation of Strains within a Family of Triaxial Tests on Overconsolidated Samples of Kaolin*, Proc. Conf. on Geotechnical Engineering, Oslo, Vol 1, 159 -163.

Table 1 Critical state parameters of some soil types [Atkinson, (1993)]

Soil	LL	PL	Typical soil parameters					
			λ	Γ	N	M	ϕ'	κ/λ
Fine-grained clay soils								
London clay	75	30	0.16	2.45	2.68	0.89	23°	0.39
Kaolin clay	65	35	0.19	3.14	3.26	1.00	25°	0.26
Glacial till	35	17	0.09	1.81	1.98	1.18	29°	0.16
Coarse-grained soils								
River sand			0.16	2.99	3.17	1.28	32°	0.09
Decomposed granite			0.09	2.04	2.17	1.59	39°	0.06
Carbonate sand			0.34	4.35	4.80	1.65	40°	0.01

Table 2 Consolidation Tests

Type	Test Number	Effective Consolidation Pressure (kPa)	Equipment	Purpose
Isotropic	IC 1-2	C : 75, 150, 300, 600 S : 600, 300, 150, 75, 15 R : 15, 75, 150, 300, 450, 600	GDS Triaxial Equipment	To establish NCL, SL and RL
Isotropic	REC01	C & S : 600 to 75 R : 75, 150, 300, 400, 500, 600 C & S : 600, 1000, 75	GDS Triaxial Equipment	To establish RL
Isotropic	REC02 REC03	C & S : 400, 75 R : 75, 150, 300, 400 C & S : 400, 600, 75 R : 75, 150, 300, 500, 600 C & S : 600, 1000, 75	GDS Triaxial Equipment	To establish RL
Anisotropic (K_0)	AC 1-2	C : 60 to 600 S : 600 to 15	GDS Triaxial Equipment	To establish K_0 NCL and SL

Notes:(i) For one-dimensional and K_0 consolidation tests, consolidation pressure is the effective axial pressure, σ'_v

- (ii)
- C - Consolidation
 - S - Swelling
 - R - Recompression
 - NCL - Normal consolidation line
 - SL - Swelling line
 - RL - Recompression line
 - K_0 NCL - K_0 normal consolidation line

Table 3 Monotonic Triaxial Tests (Isotropic)

Test Number	Cell Pressure (kPa)	Initial Back Pressure (kPa)	Final Back Pressure (kPa)	Final Effective Consolidation Pressure (kPa)	OCR	Test Type
MIC011	300	200	200	100	1	Compression
MIC012	300	200	200	100	1	-
MIC013	400	200	200	200	1	-
MIC014	400	200	200	200	1	-
MIC015	600	200	200	400	1	-
MIC017	800	200	200	600	1	-
MIC018	800	200	200	600	1	-
MIC021	800	200	500	300	2	-
MIC041	800	200	650	150	4	-
MIC042	800	200	650	150	4	-
MIC401	800	200	785	15	40	-
MIC402	800	200	785	15	40	-
MIE011	300	200	200	100	1	Extension
MIE013	400	200	200	200	1	-
MIE015	600	200	200	400	1	-
MIE017	800	200	200	600	1	-
MIE021	800	200	500	300	2	-
MIE041	800	200	650	150	4	-
MIE401	800	200	785	15	40	-

Table 4 Monotonic Triaxial Tests (Anisotropic)

Test Number	Initial Effective Cell Pressure (kPa)	Initial Effective Axial Pressure (kPa)	Final Eff Cell Pressure (kPa)	Final Eff. Axial Pressure (kPa)	Final Mean Normal Effective Stress, p' (kPa)	OCR	Test Type
MAC011	52	100	52	100	68	1	Compression
MAC013	104	200	104	200	136	1	-
MAC015	208	400	208	400	272	1	-
MAC017	312	600	312	600	408	1	-
MAC021	312	600	156	300	204	2	-
MAC041	312	600	78	150	102	4	-
MAC401	312	600	8	15	10	40	-
MAE011	52	100	52	100	68	1	Extension
MAE013	104	200	104	200	136	1	-
MAE015	208	400	208	400	272	1	-
MAE017	312	600	312	600	408	1	-
MAE021	312	600	156	300	204	2	-
MAE041	312	600	78	150	102	4	-
MAE401	312	600	8	15	10	40	-

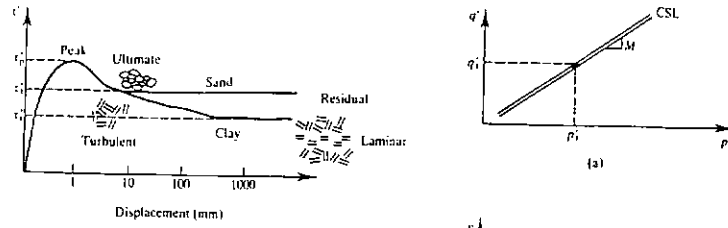


Figure 1 Residual strength of clay at very large displacements

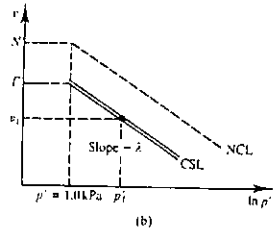
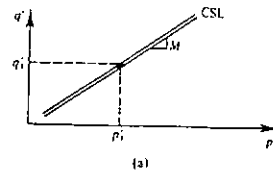


Figure 2 Critical state line for triaxial tests



Figure 3 GDS equipment

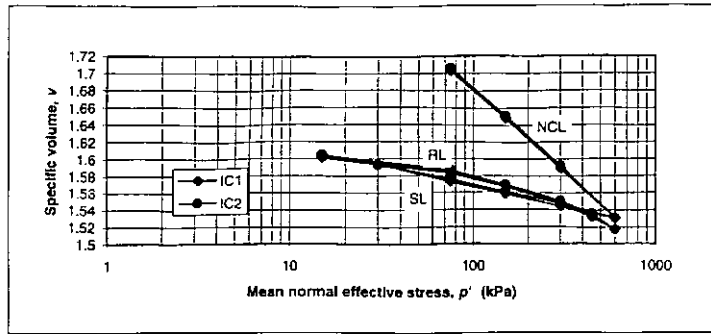
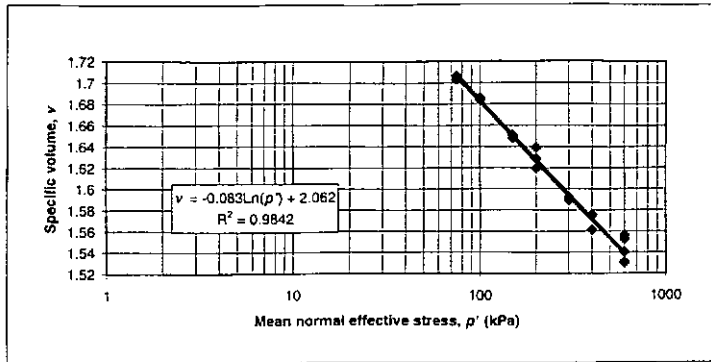
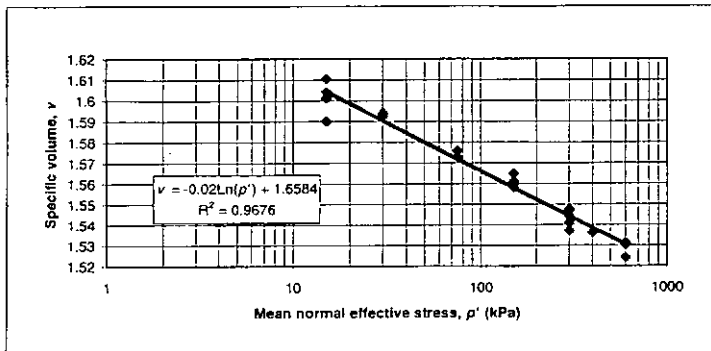


Figure 4 Specific volume versus mean normal effective stress from isotropic consolidation tests

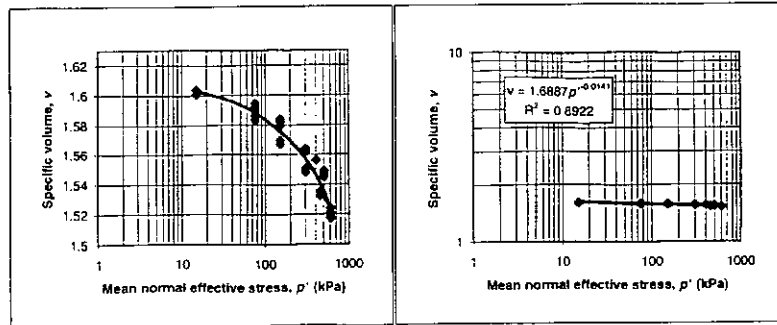


(a) Normal consolidation line



(b) Swelling line

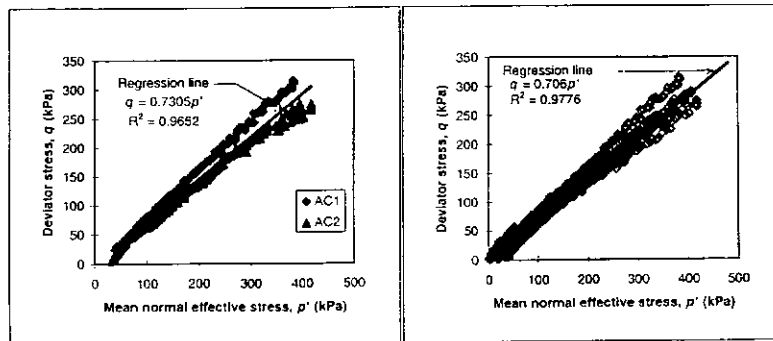
Figure 5 Normal consolidation line and swelling line from isotropic consolidation tests



(a) in $v - \ln p'$ space

(b) in $\ln v - \ln p'$ space

Figure 6 Recompression line from isotropic consolidation tests



(a) Regression results from initial K_0 consolidation tests

(b) Regression results from all K_0 consolidation tests

Figure 7 K_0 consolidation line in $q - p'$ space

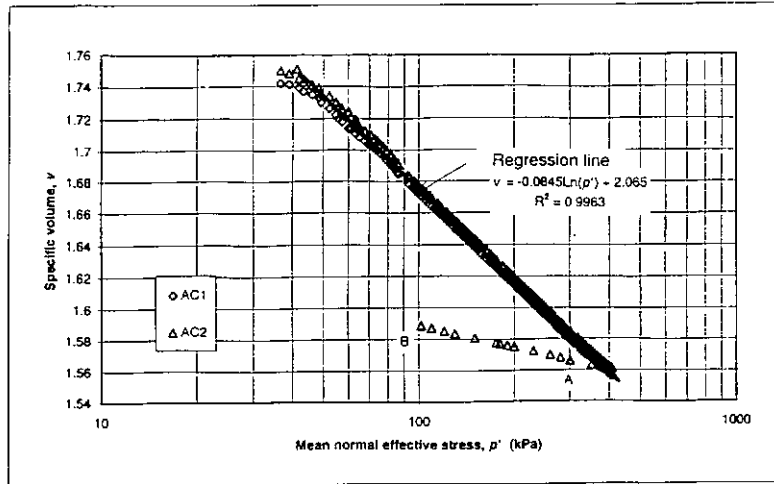


Figure 8 Normal consolidation line from K_0 consolidation tests (K_0 NCL)

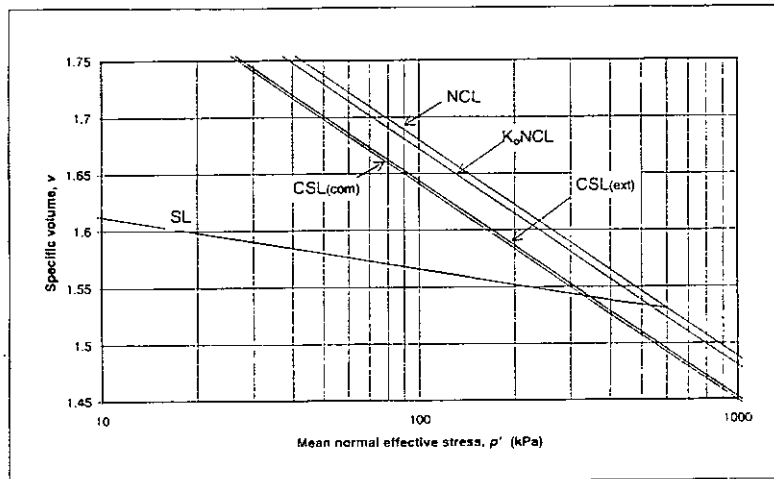
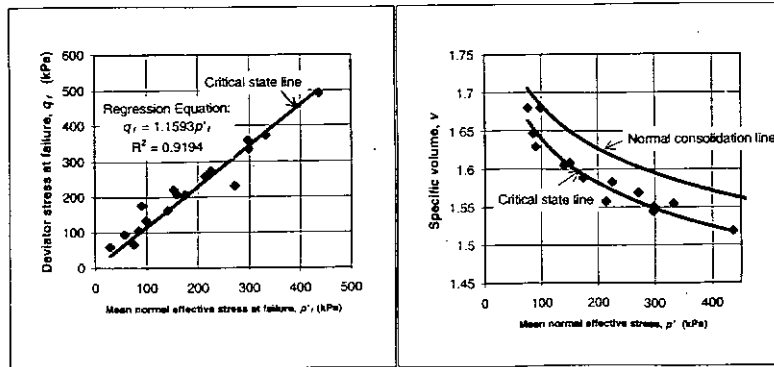


Figure 9 Specific volume versus mean normal effective stress



(a) q_f vs p'_f

(b) v vs p'

Figure 10 Failure points for CU compression tests on isotropically and anisotropically consolidated specimens of all stress histories

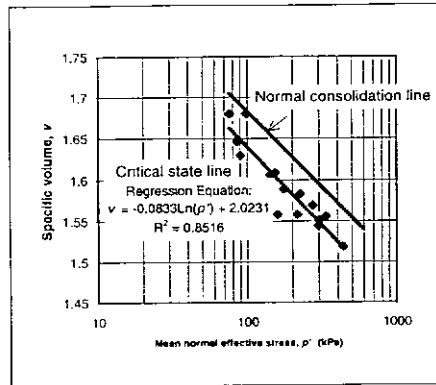
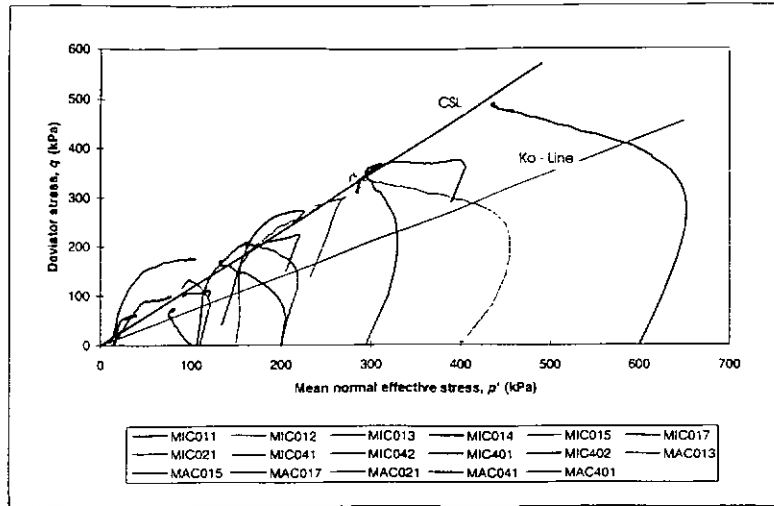
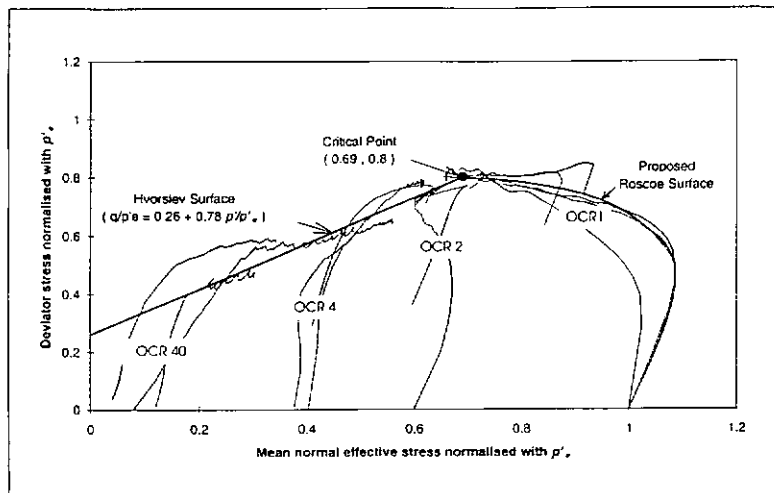


Figure 11 The critical state line in $v - \ln p'$ space (Compression)



(a) in $q - p'$ space



(b) in $q/p'_{*} - p'/p'_{*}$ space

Figure 12 Effective stress paths from CU compression tests

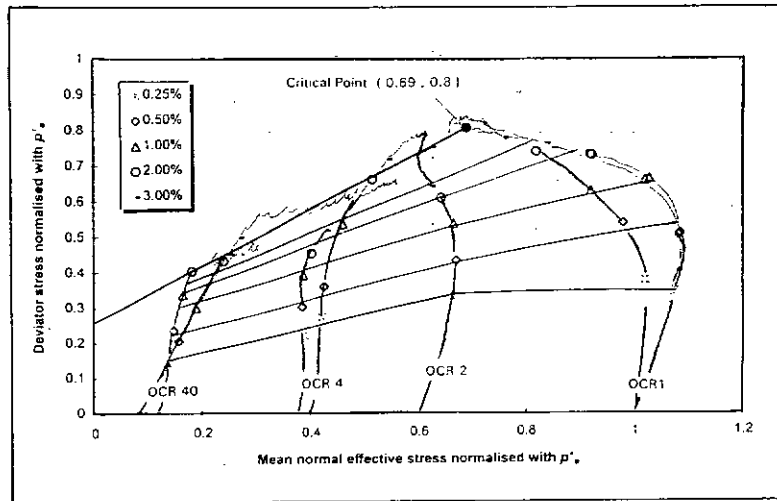


Figure 13 Strain contours - CU compression tests on isotropically consolidated specimens

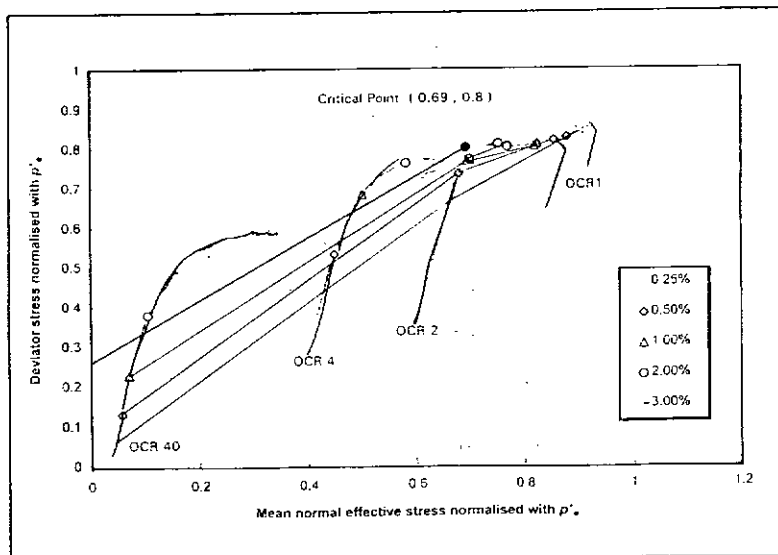
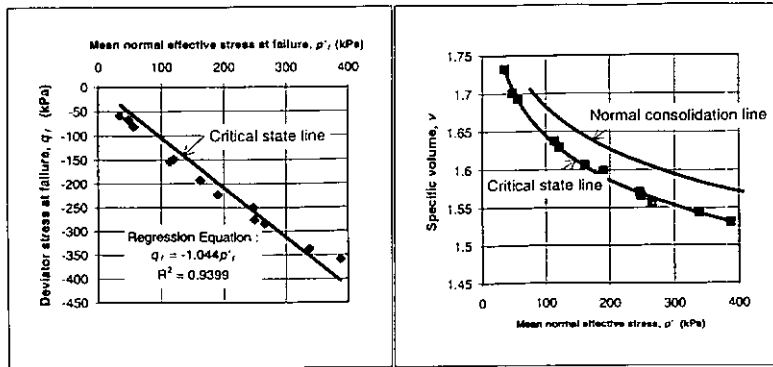


Figure 14 Strain contours - CU compression tests on anisotropically consolidated specimens



(a) q_f vs p'_f

(b) v vs p'

Figure 15 Failure points for CU extension tests on isotropically and anisotropically consolidated specimens of all stress histories

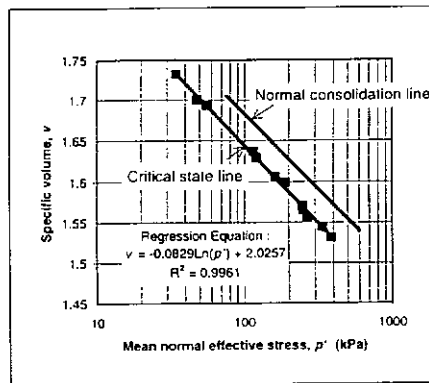
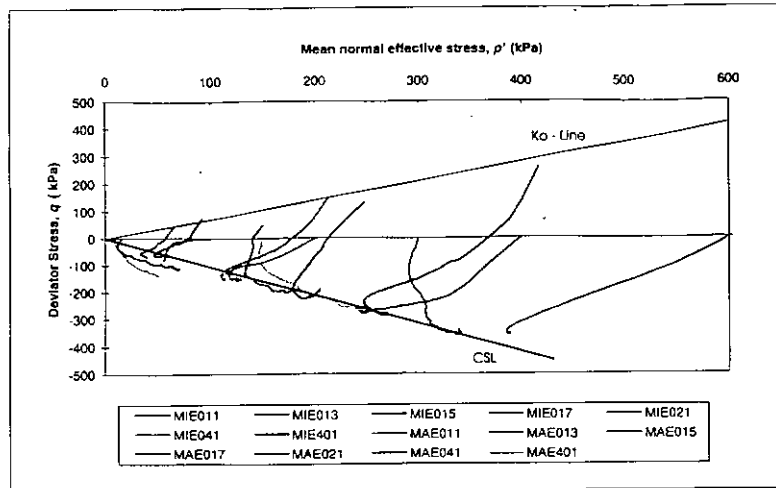
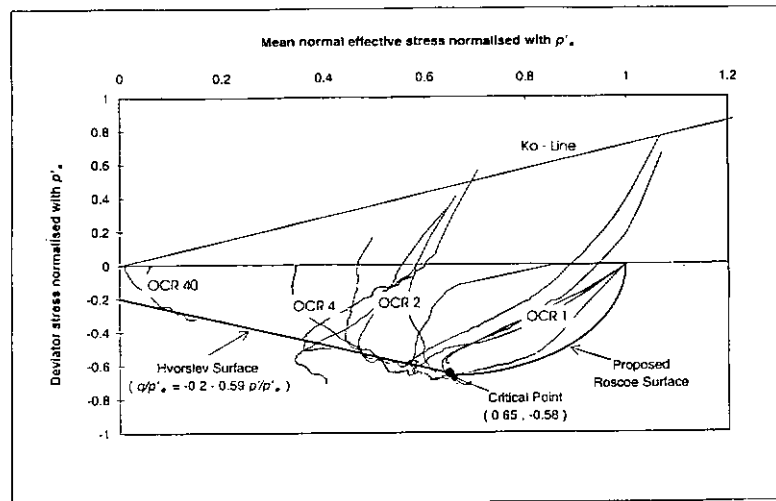


Figure 16 The critical state line in $v - \ln p'$ space (Extension)



(a) in $q - p'$ space



(b) in $q/p' - p'/p'$ space

Figure 17 Effective stress paths from CU extension tests

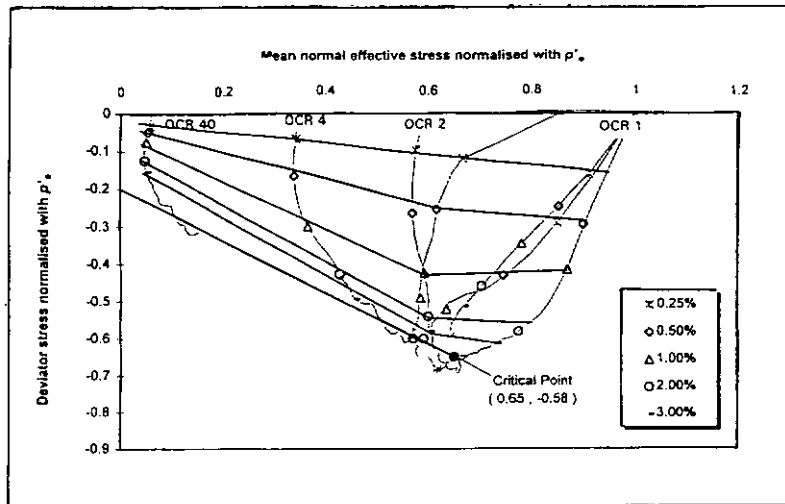


Figure 18 Strain contours - CU extension tests on isotropically consolidated specimens

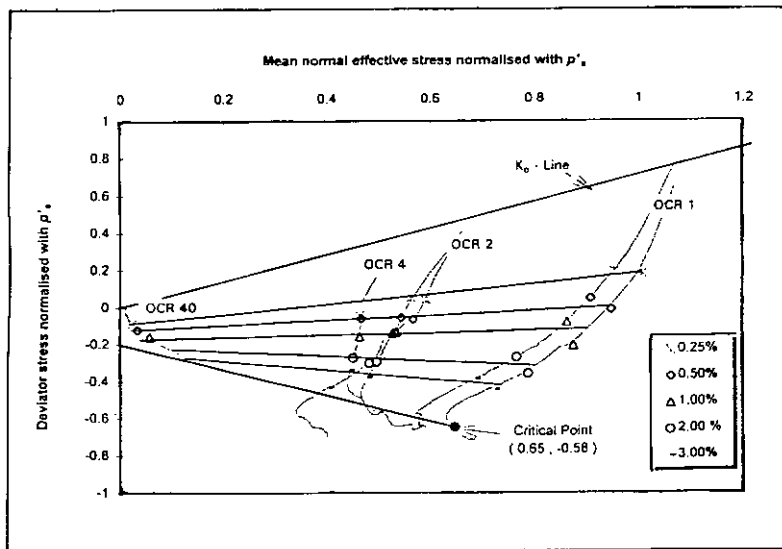


Figure 19 Strain contours - CU extension tests on anisotropically consolidated specimens

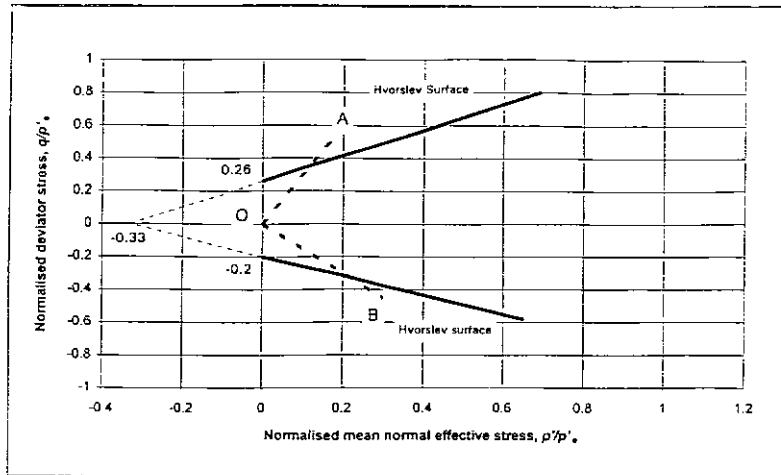


Figure 20 Hvorslev and no-tension surfaces from CU compression and extension tests

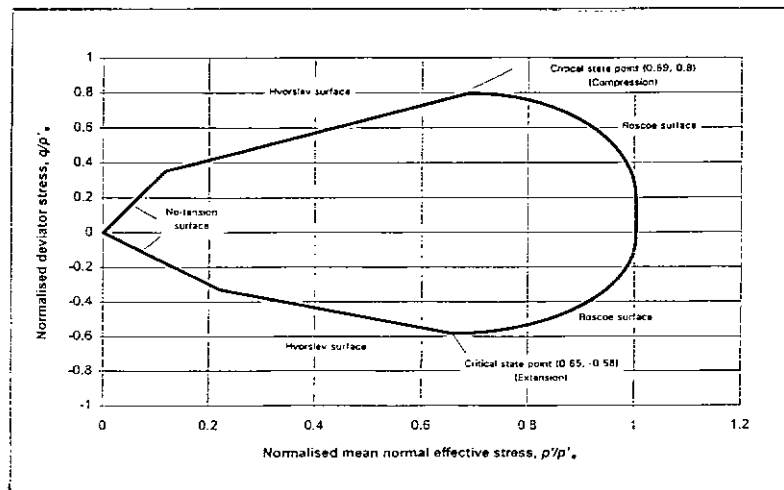


Figure 21 Critical state boundary surface for Kauper Marl silt